Optical absorption measurements in a new composite material by combined photoacoustic and beam transmission techniques

C. L. Cesar, C. A. S. Lima, N. F. Leite,[a] and H. Vargas
Instituto de Física, UNICAMP 13100, Campinas, S. Paulo, Brazil

A. F. Rubira[b] and F. Galembeck
Instituto de Química, UNICAMP 13100, Campinas, S. Paulo, Brazil

(Received 6 August 1984; accepted for publication 10 October 1984)

The absorption coefficient of a highly absorbing ($\beta > 10^5$ cm^{-1}) new composite produced in our laboratory, namely manganese dioxide surface-impregnated polyethylene (MnO_2–PE) film, has been measured in the visible range. We have employed a combination of concurrently taken photoacoustic and beam transmission data. This combination proved to be an effective means for the optical evaluation of highly absorptive samples which dispenses with the need for prior knowledge of the sample reflectivity. Theoretical interpretation of MnO_2–PE absorption profile, with due account of the processes underlining the photoacoustic signal generation, reveals a semiconductor behavior with an estimated effective gap wavelength of 8050 Å. Technical implications of the availability of these highly absorptive flexible films are briefly considered.

I. INTRODUCTION

In recent years a number of techniques has been advanced for polymer surface modification, with important established or potential technological impact.[1–9] For chemically inert low surface energy polymers, surface impregnation with metal oxides has been achieved by *in situ* oxidation of presorbed metalorganic complexes.[5–9] However when the polymer structure itself provides reduction sites, manganese oxide incorporation can be shown to proceed directly under the action of an acidic, oxidizing potassium permanganate solution. We have shown this to be the case with polyethylene (PE) and have obtained highly adherent surface coatings of MnO_2 onto PE samples.

It immediately became apparent to us that MnO_2–PE thin films were suited for a number of interesting technical applications. We thus decided to proceed a thorough investigation of its physical properties, e.g., its optical absorptivity. The point was that after a few preliminary essays this new composite proved to have an exceptionally high absorption coefficient (β) throughout the visible range. However, difficulties in measuring large β's with standard techniques are well known to those working on materials characterization problems. One way out is to use photacoustics (PA), a technique whose possibilities can be appreciated from some recent reviews of the subject and its applications.[10–12]

In this paper, together with a summary description of the metal oxide-on-polymer thin film obtention, a procedure is described which explores a combination of spectroscopic data from both PA and transmission measurements.

II. EXPERIMENT

A. Composite obtention

An account of some of the problems involved in obtaining polymer surface modification, e.g., the preparation of polymer supported metal oxide thin films, can be found elsewhere.[9] Here we shall concentrate on those details which are of relevance to characterize the parameters controlling the production of MnO_2–PE film through the application of our new methodology.

The supporting PE films were obtained from commercially available, low density, blown polyethylene films, 33 μm thick. The identity of PE was checked by infrared spectroscopy. Picnometry determined mass density was 0.933 g cm^{-3} at 25 °C. Water was redistilled from an alkaline solution of $KMnO_4$ in a glass still. Other chemicals used were reagent grade.

Oxidation experiments were carried according to the following scheme: (a) PE samples were initially carefully cleaned by soaking them in detergent, then thoroughly rinsed in water and ethanol, wiped off with tissue paper, and finally oven dried at 60 °C for 1 h. (b) Samples were then exposed (one face only) to an acidic oxidizing solution (0.01 M $KMnO_4$, 0, 20 M H_2SO_4); a thermostabilized bath kept the oxidation temperature constant at 70 °C throughout the operation. (c) To acquire different coating thicknesses, the oxidation times were varied; for our measurements, samples were prepared with oxidation times of 30, 60, 240, and 480 min. (d) Following oxidations, the samples were thoroughly rinsed in water, rubbed with lintless cloth to remove nonadhered scraps, and then oven dried for 1 h at 60 °C.

TABLE I. Thickness of deposit for the surface impregnated MnO_2 on PE samples as a function of the oxidation time: values were determined by mass change measurements (average over three determinations), except for sample (a) for which the quoted value was obtained from consistency fits (see the text for details).

Sample	Oxidation time (min)	MnO_2 deposit thickness (nm)
(a)	30	17.5 ± 0.8
(b)	60	38 ± 7
(c)	240	91 ± 15
(d)	480	183 ± 20

[a] On leave of absence from Physics Department, Universidade Estadual Paulista, Guaratinguetá, S. Paulo, Brazil.
[b] On leave of absence from Chemistry Department, Universidade Estadual de Maringá, Paraná, Brazil.

 0021-8979/85/094431-06$02.40

As mentioned above, samples were produced with different oxidations times. To obtain the corresponding thicknesses we proceeded as follows: (1) disk-shaped pieces of surface modified PE films were cut, the area and mass being carefully determined. (2) Complete removal of the MnO_2 coatings was achieved with a 3.0 N solution of HCl followed by water rinsing, wiping off with tissue paper, and oven drying at 60 °C, to reach constant mass. (3) Comparing the masses found in steps (1) and (2) allowed for determination of oxide mass and thereby its average thickness could be simply calculated from the additional knowledge of its mass density. In Table I we present, as function of the oxidation time, the thickness of the oxide deposits thus obtained.

B. Absorption measurements

PA measurements were carried using a standard setup comprising a modulated light source (Oriel Model 6269 lamp with PAR Model 191 variable frequency light chopper), a Jarrel–Ash Model 82-020 spectrometer, a PAR Model 119 lock-in amplifier, a XY register, and a homemade high gain PA cell fited with a high sensitivity Brüel and Kjäer Model 4166 microphone. Cell window had a high transparency throughout our working wavelength range and the sample holder could be easily removed from the cell. Disk-shaped samples of MnO_2–PE, prepared as described above, could also be placed (removed), without damage into (from) the sample chamber in the holder PA. Signal processing followed, with pyroelectric normalization. To this end, the lamp-blank spectrum was acquired pyroelectrically and intensity variations were accounted for using standard PA normalization procedures.[10]

For the transmission measurements, transmitted beam intensities data were also acquired using pyroelectric detection (Molectron P1 Series). After PA measurements at all wavelengths were taken, the sample holder was removed. The light beam after passing through the PA cell window reached the sample (already removed from the PA holder and placed in the light path) and through it onto the detector. Signal processing went through as with PA processing. This procedure ensured that the PA and transmission data were acquired under essentially the same sample excitation conditions. A schematic of the experimental setup is shown in Fig. 1.

III. METHODOLOGY

Along the past years we have explored different uses of the PA techniques.[13–20] In particular, we have taken advantage of its suitability to work with solids or liquids which, for one reason or another, could hardly be measured using conventional methods. It seemed thus well suited for the spectroscopic evaluations we wanted to perform. However, we soon observed that, with the material we had at hand, PA by itself would not do. It happens that when the sample reflectivity $R(\lambda)$ cannot be neglected, even PA meets with difficulty to isolate $\beta(\lambda)$[10,12] because the light intensity entering the sample depends of R. Also, for such strong an absorber as MnO_2–PE, photoacoustic saturation poses a problem[10,12,21] which has to be coped with. In fact, even samples with finely divided particles would still be rendered optically opaque, though thermally thin, unless thickness was drastically reduced.[21] The point here is that according to the widely accepted Rosencwaig–Gersho theory,[10,22] for the PA effect, such samples are photoacoustically opaque, unless the thermal diffusion length μ is made smaller than the optical absorption length β^{-1}. This would, however, require going into the kHz range of modulation frequencies (ω) since $\mu \propto \omega^{-1/2}$ unless, we repeat, we got down to extremely thin, highly uniform, well adhered coatings. This is what we have accomplished in preparing MnO_2–PE films with very thin (down to ~ 100 Å) uniform strongly adhered (no peel off) MnO_2 surface coatings. As we shall see below, a combination of concurrently acquired PA and transmission data solved the aforementioned difficulty of not knowing $R(\lambda)$, and we were thus able to determine with good accuracy and reproducibility the optical absorption coefficient for MnO_2–PE using adequate samples. In fact, we worked with samples where the MnO_2 coatings were thin enough to avoid photoacoustic saturation and to allow transmitted beam intensities to be comfortably detected with a high, sensitivity pyroelectric detector, in our transmission measurements. We should also mention that we were strongly motivated by the fact that, in regards to the intense contemporary quest[23,24] for highly flexible, self-supported, efficient absorbers for solar collector lining and similar applications, MnO_2–PE seems to meet well with the overall expectations.

As we stated above, we set out to measure, for wavelengths λ in the visible range, the optical absorption coefficient $\beta(\lambda)$ for the MnO_2–PE composite. Our determinations

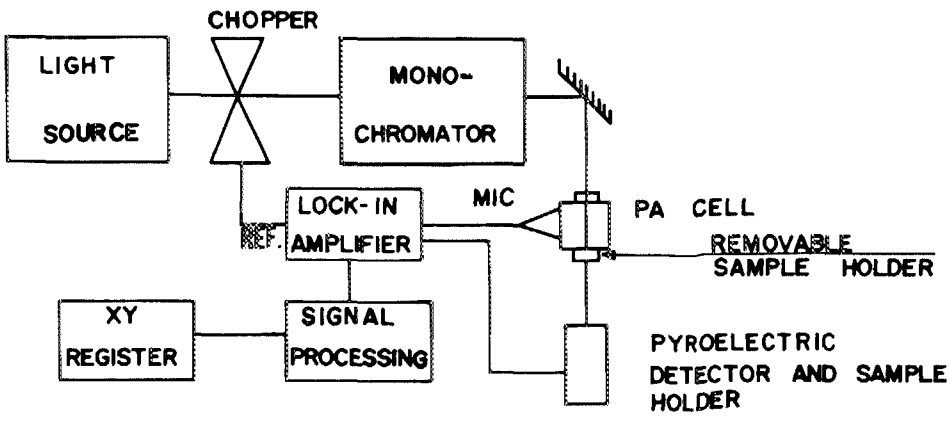

FIG. 1. Experimental setup.

should be based on samples which were identical except for the thickness of the surface coating, due to different times of exposure to impregnation, as we described above. The full dependence of both the PA signal and beam attenuation on the wavelength λ, which comes about through both the absorption coefficient $\beta(\lambda)$ and the sample reflectivity $R(\lambda)$ should be taken into account. We had thus to circumvent the difficulty of $R(\lambda)$ being unknown for the samples.

For a solid sample of thickness l, reflectivity $R(\lambda)$, and absorption coefficient $\beta(\lambda)$, the transmitted beam intensity $T(\lambda)$ and the photoacoustic signal $S(\lambda)$ can be represented, with explicit account of all λ-dependent terms, as follows[10,12,15]:

$$T(\lambda) = A_0[1 - R(\lambda)]\exp[-\beta(\lambda)l], \tag{1}$$

$$S(\lambda) = B_0[1 - R(\lambda)][1 - \exp(1 - \beta(\lambda)l)]. \tag{2}$$

When both photoacoustic and transmitted intensity data are concurrently avaliable the two signals can be combined into

$$S(\lambda) = a(\lambda) - bT(\lambda), \tag{3}$$

where

$$a(\lambda) = [1 - R(\lambda)]B_0 \quad \text{and} \quad b = B_0/A_0, \tag{4}$$

i.e.,

$$T(\lambda) = (a/b)\exp[-\beta(\lambda)l] \tag{5}$$

and

$$S(\lambda) = a\{1 - \exp[-\beta(\lambda)l]\}. \tag{6}$$

Here b is a constant and a depends on λ through $R(\lambda)$, as given by Eq. (4)

IV. RESULTS AND DISCUSSION

Our measurements produced the photoacoustic $[S(\lambda)]$ and transmission $[T(\lambda)]$ spectra depicted in Figs. 2 and 3, for our various samples. In Fig. 4 we plot $S(\lambda)$ vs $T(\lambda)$. We have performed a computer search based on the data in Fig. 4, for a relationship between $S(\lambda)$ and $T(\lambda)$ using a least-squares fit to polynomial functions of up to third degree. Our results indicate that a linear relationship fits the data best for all samples. The superimposed straight lines in Fig. 4 represent, accordingly, the best fit (minimum χ^2) through the data. This linear relation between $S(\lambda)$ and $T(\lambda)$, led us to conclude that the parameter a in Eqs. (3)–(6) shows little dependence on λ, the same being true, of course, for $R(\lambda)$ throughout the visible range. As to the solid lines shown in Figs. 2 and 3, they represent $S(\lambda)$ and $T(\lambda)$ for each sample, as computed using Eqs. (5) and (6), by setting $a = \bar{a}$, $b = \bar{b}$, and $\beta(\lambda) = \bar{\beta}(\lambda)$ whose values were determined as follows. Equations (5) and (6) were inverted to give $\beta(\lambda)$ independently:

$$\beta_T(\lambda) = (1/l)\ln\{\bar{a}/[\bar{b}(\lambda)]\}, \tag{7}$$

$$\beta_S(\lambda) = (1/l)\ln\{1 - [S(\lambda)/\bar{a}]\}^{-1}, \tag{8}$$

where the samples thicknesses l are given in Table I: $\bar{a}$ and $\bar{b}$ mean the value of a, b obtained through the linear fits and are collected in Table II, for samples (a) thru (d). With these values and the experimentally determined $S(\lambda)$ and $T(\lambda)$, we used Eqs. (7) and (8) to obtain $\beta_T(\lambda)$ and $\beta_S(\lambda)$, where the subscripts stand as reminders of the measured data used on each point-by-point calculation of the corresponding $\beta(\lambda)$. Of course, for a given λ, $\beta_T(\lambda)$ and $\beta_S(\lambda)$ should coincide, within experimental error, and should be independent of the sample thickness l. We can thus take as the sample absorption coefficient at each λ the average value

$$\bar{\beta}(\lambda) = (1/2N)\sum_{ij}\beta_{ij}(\lambda), \tag{10}$$

where $\beta_{ij}(\lambda)$ is the value of $\beta(\lambda)$ determined for sample i by using the jth measurement technique. Thus, i runs from $i = 1$ to $N =$ number of different sample thicknesses used while $j = 1$ for transmission (T), $j = 2$ for photoacoustic (S) technique. Actually, for reasons to be explained later, for this average only samples (b) through (d) were considered. We have also computed $\delta\beta(\lambda)$, the standard deviation from the mean for all β's and found $(\delta\beta/\beta)$, throughout our range of λ, not to exceed a few percent. This result entirely sup-

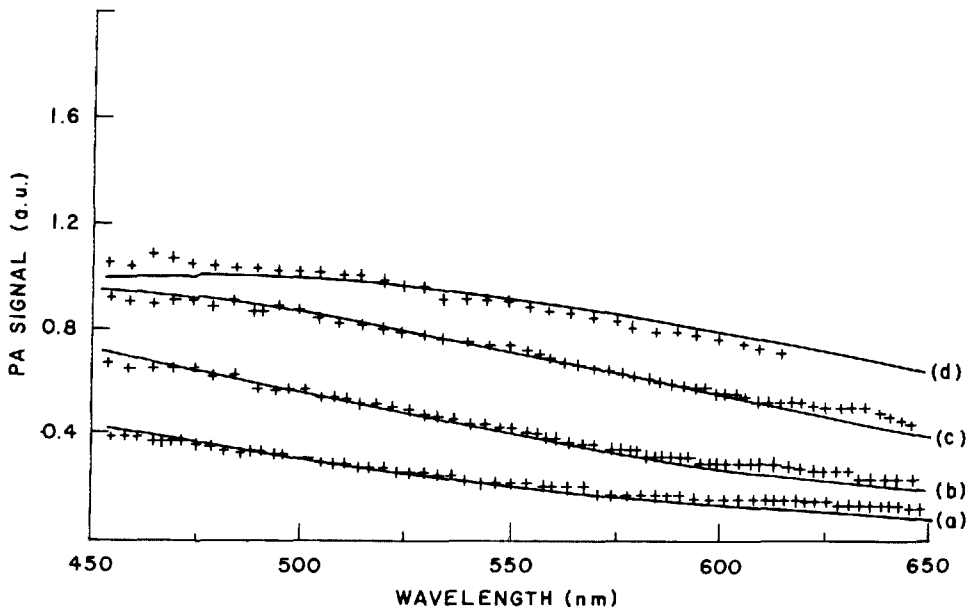

FIG. 2. Photoacoustic spectra for the various MnO_2–PE samples (labels correspond to those in Table I).

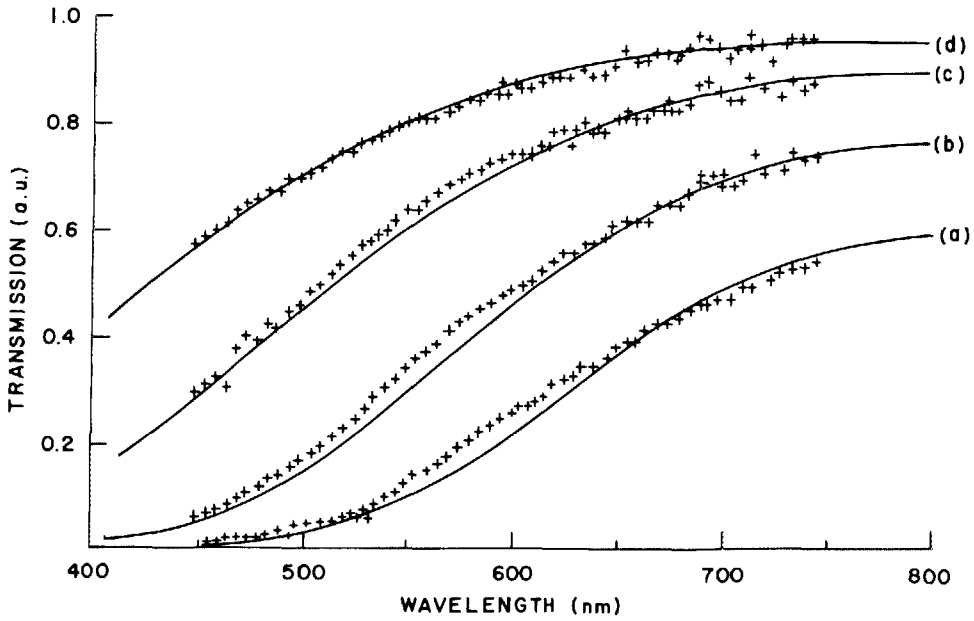

FIG. 3. Transmission spectra for the various MnO_2–PE samples (labels correspond to those in Table I).

ports the consistency of our procedure. A plot of $\bar{\beta}(\lambda)$ vs λ is given in Fig. 5. Here we can appreciate the exceptionally high value of $\bar{\beta}(\lambda)$ for this new composite MnO_2–PE, ranging from ~ 1.0 to $3.2\times10^5\ cm^{-1}$ for λ going from 650 to 450 nm, respectively.

Two points should be remarked here, as regards to our determination of $\beta(\lambda)$. First, one could expect some contribution to the signal in the PA measurements and to the beam attenuation in the transmission measurements, arising from the polyethylene substrate. To check this we have used nonimpregnated PE samples. We found that in our range of λ's, the corrections were always below 10% and essentially independent of λ, so that the value of $\bar{\beta}(\lambda)$ reported above can be safely assigned to the MnO_2 coating itself, within 10% experimental error. This uncertainty also easily accommodates the marginal effects on the PA measurements arising from residual absorption within the PA cell of reflected and transmitted light. Second, our appreciation of the $\bar{\beta}(\lambda)$ curve led us to consider the presence of a band gap below 700 nm. The possibility was apparent that the MnO_2 layer was exhibiting an amorphous or polycrystalline semiconductor behavior. We took the $\bar{\beta}(\lambda)$ data and found it to fit rather well ($\chi^2 < 5\times10^{-5}$) a parabola when plotted against the inverse of λ. This is consistent with

$$\beta(\lambda) = \alpha[(1/\lambda) - (1/\lambda_g) + C]^2 \tag{11}$$

to be expected for either indirect gap or heavily doped semiconductors.[25] It should be remarked further that independently carried out investigations of the state of the MnO_2 surface layer on PE led to the conclusion that manganese + oxygen combination on the surface of the polymer is probably nonstoichiometric, being described as MnO_{2-x}, with x ranging between 0 and 0.3. Thus, the possibility cannot be discarded of self-diffusing defects (impurities) within the surface crystallites.

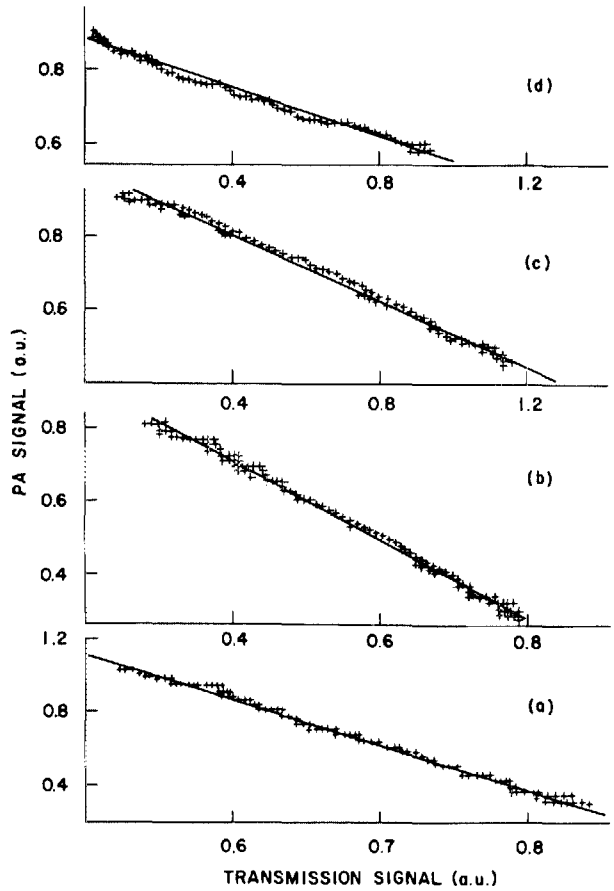

FIG. 4. Correlation between photoacoustic and transmission spectra for the various MnO_2–PE samples (labels correspond to those in Table I).

TABLE II. The fitted values of the parameters $\bar{a}$ and $\bar{b}$ obtained from least-squares fits to a straight line in the plots of $S(\lambda)$ vs $T(\lambda)$ (Fig. 4).

Sample	$\bar{a}$	$\bar{b}$
(a)	2.32 ± 0.01	2.44 ± 0.02
(b)	1.14 ± 0.01	1.08 ± 0.01
(c)	0.98 ± 0.01	0.45 ± 0.01
(d)	0.88 ± 0.01	0.33 ± 0.01

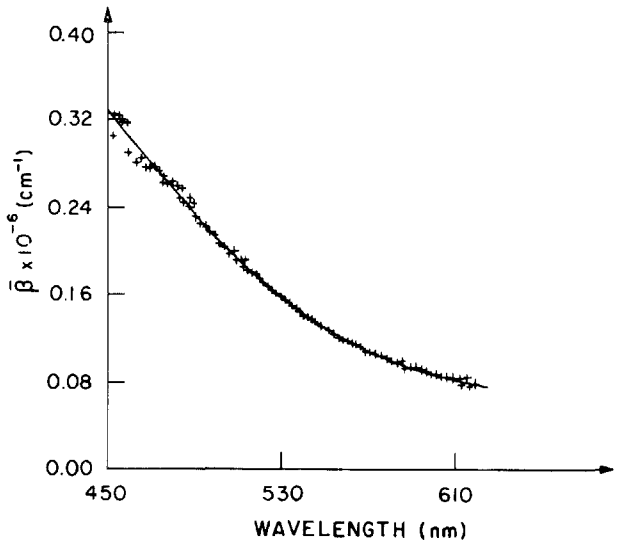

FIG. 5. The absorption coefficient for the new composite: manganese dioxide surface impregnated polyethylene (MnO_2–PE).

As we have mentioned, a fit was made of the $\bar{\beta}(\lambda)$ data to the function $K_0 + K_1(1/\lambda) + K_2(1/\lambda^2)$. The least-squares fitted parameters (with a $\chi_2 < 10^{-4}$) were (for $1/\lambda$ in units of $1000\,\text{nm}^{-1}$): $K_0 = 0.50$, $K_1 = -0.79$, and $K_2 = 0.32$. Then, with the normally met condition $C \ll 1/\lambda$, we have from Eq. (11) after comparison with the fitted polynomial: $\alpha = K_2$, $\lambda_g = (-2K_2/K_1) \times 10^3$ nm, and also $\lambda_g = K_2/K_0)^{1/2} \times 10^3$ nm. These two independent determinations of λ_g give the values 810 and 800 nm, respectively. Thus we can quote for our determination of the effective gap wavelength for MnO_2 coating in MnO_2-PE the average value $\lambda_g = 805$ nm.

Before closing this section, we should like to make a remark concerning the MnO_2 film thickness. As given in Table I, the l values of samples (b) through (d) were worked out from the measurement of the PE substrate mass change upon surface impregnation with MnO_2. However, in the course of our analysis, we noticed that the $\beta_S(\lambda)$ vs $\beta_T(\lambda)$ correlation for sample (a) was rather poor in comparison with the very good linear correlation found for samples (b) through (d). On account that samples (a) through (d) differed solely on the MnO_2 deposit thicknesses, we suspected that the value of l obtained for sample (a) was in large error. Accordingly, we decided to obtain $\bar{\beta}(\lambda)$ using Eq. (10) for samples (b) through (d) only. Then, with this value of $\bar{\beta}(\lambda)$ we took Eqs. (7) and (8) to get an average value for l_a the thickness of sample (a). The value found was $l_a = 17.5$ nm. Then we went back and with this new value of l_a we checked again the linear correlation between $\beta_S(\lambda)$ and $\beta_T(\lambda)$ for this sample and found it to be just as good now as for the other samples. We can point out some possible reasons for such a discrepancy in the estimates of sample (a) thickness by the independent procedures just quoted. First, recall from Table I that this sample is the thinnest one. For one thing it would be more critically affected by nonuniformities on the surface properties of the substrate (PE film) which would reflect quite strongly on an invalidation of the underlying hypothesis of surface uniformity of the coating, which is basic to the calculated estimate of the sample average thickness.

For thicker layers this effect would of course be less critic. Indeed, thicker MnO_2 deposits on PE are rather uniform as evidenced by iridescence and scanning electron microscope examination. However, thinner deposits (for which we do not, at this point, have any morphological data) may well be nonuniform, due to localization of nucleation sites in PE substrate. Also there is some evidence that MnO_2 layers closer to the substrate differ from the others; upper layers, in some respects. Absorption behavior would then reflect this change in MnO_2 characteristics as oxide formation proceeds.

V. SUMMARY AND CONCLUSIONS

We have reported on the determination of the absorption profile $\beta(\lambda)$ for the new composite MnO_2–PE. We have found $\beta(\lambda)$, in the visible range, to exhibit very high values, of the order of 10^5 cm^{-1}. Our determinations used a combination of PA and transmission data. To make measurements possible, i.e., to avoid complete opacity and photoacoustic saturation, samples had to be produced with very thin coatings (1800 down to ~ 100 Å). This was made possible by the now available polymer oxide coating techniques. Our results on $\beta(\lambda)$ for the MnO_2–PE composite is consistent with that of a semiconductor (amorphous or polycrystalline) with an estimated effective gap wavelength of 8050 Å. To check further on this, work is under way to proceed a thorough evaluation of the effective gap dependence on the surface impregnation parameters and on the techniques for polymer surface modification, as well as to carry on measurements the composite electrical conductivity as function of temperature and will be reported elsewhere.

We have also briefly commented above on the potential of MnO_2–PE as a possible light absorber material for use in the lining of solar collectors, as well as in other related applications. These aspects are currently under test in our laboratory and an evaluation of this new composite photothermal efficiency will soon be communicated.

ACKNOWLEDGMENTS

This work is carried under support from a STI/MIC grant to UNICAMP, Contract 025/83. NFL and AFR acknowledge fellowships from Coordenação de Aperfeiçoamento de Pessoal de Nível Superion-CAPES through the PICD program. CASL and HV acknowledge Research Professorships from CNPq-Brazil.

[1] D. W. Dwight and W. M. Riggs, J. Colloid Interface Sci. **47**, 650 (1974).
[2] J. T. Kenney, W. . Townsend, and J. A. Emerson, J. Colloid Interface Sci. **42**, 589 (1973).
[3] G. C. S. Collins, A. C. Lowe, and D. Nicholas, Eur. Polym. J. **9**, 1173 (1973).
[4] J. Jansta, F. P. Dousek, and J. Riha, J. Appl. Polym. Sci. **19**, 3201 (1975).
[5] F. Galembeck, J. Polym. Sci. Polym. Lett. Ed. **15**, 107 (1977).
[6] F. Galembeck, S. E. Galembeck, H. Vargas, C. A. Ribeiro, L. C. M. Miranda, and C. C. Ghizoni, in *Surface Contamination*, edited by K. L. Mittal (Plenum, New York, 1979), p. 54.
[7] F. Galembeck, J. Polym. Sci. Polym. Chem. Ed. **16**, 3015 (1978).

[8]F. Galembeck, C. C. Ghizoni, C. A. Ribeiro, H. Vargas, and L. C. M. Miranda, J. Appl. Polym. Sci. **25,** 1427 (1980).
[9]R. Baumhardt-Neto, S. E. Galembeck, I. Jockes, and F. Galembeck, J. Polym. Sci. Polym. Chem. Ed. **19,** 819 (1981).
[10]A. Rosencwaig, *Photoacoustics and Photoacoustic Spectroscopy* (Wiley, New York, 1980).
[11]J. B. Kinney and R. H. Staley, Annu. Rev. Mater. Sci. **12,** 295 (1982).
[12]J. F. McClelland, Anal. Chem. **55,** 89 (1983).
[13]C. C. Ghizoni, M. A. Siqueira, H. Vargas, and L. C. M. Miranda, Appl. Phys. Lett. **32,** 554 (1978).
[14]C. L. Cesar, H. Vargas, J. A. Meyer, and L. C. M. Miranda, Phys. Rev. Lett. **42,** 1570 (1979).
[15]C. A. S. Lima and L. C. M. Miranda, Phys. Lett. A **79,** 215 (1980).
[16]C. A. S. Lima, L. C. M. Miranda, and R. Santos, J. Appl. Phys. **52,** 137 (1981).
[17]R. Florian, J. Pelzl, M. Rosenberg, H. Vargas, and R. Wernhardt, Phys. Status Solidi A **48,** K35 (1978).
[18]C. A. S. Lima, J. C. V. Mattos, L. C. M. Miranda, A. S. F. Penna, J. Bulow, and C. C. Ghizoni, J. Photoacoust. **1,** 61 (1982).
[19]C. Evora, R. Landers, and H. Vargas, Appl. Phys. Lett. **36,** 864 (1980).
[20]C. L. Cesar, H. Vargas, C. A. S. Lima, J. Mendes Filho, and L. C. M. Miranda, J. Agric. Food Chem. (in press).
[21]J. W. Lin and L. P. Dudek, Anal. Chem. **51,** 1627 (1979).
[22]A. Rosencwaig and A. Gersho, J. Appl. Phys. **47,** 64 (1976).
[23]S. Gross, Editor, Modern Plastics (Design & Application News) **14,** 30 (1984).
[24]O. P. Agnihotri and B. K. Gupta, *Solar Selective Surfaces* (Wiley, New York. 1981).
[25]J. I. Pankove, *Optical Processes in Semiconductors* (Dover, New York, 1975), pp. 37–40.